Aerosol and Air Quality Research

ORIGINAL RESEARCH
https://doi.org/10.4209/aaqr.2020.04.0146

Refined Source Apportionment of Atmospheric $PM_{2.5}$ in a Typical City in Northwest China

Yiting Wang[1,2], Yong Zhang[1,2], Xia Li[1,2], Junji Cao[1*]

[1] Key Laboratory of Aerosol Chemistry & Physics (KLACP), Institute of Earth Environment, Chinese Academy of Sciences, Xi'an 710061, China
[2] University of Chinese Academy of Science, Beijing 100049, China

ABSTRACT

The Xixian New District (XXND), established in 2014, is the seventh national-level new district in China, but research on air pollution there has been limited. This study focused on the characteristics and sources of $PM_{2.5}$ in XXND from 2017 to 2018. The average annual $PM_{2.5}$ mass was 67 μg m^{-3}; loadings were high in winter and low in summer. Organic carbon (18.2%), nitrate (17.0%), and sulfate (13.1%) were the main chemical components of $PM_{2.5}$. A refined statistical assessment of sources was conducted using the CAS-HERM receptor model, and it showed that primary sources accounted for ~58.5% of the $PM_{2.5}$ annual mass, of which dust accounted for 23.3% (road, construction, and soil dust accounted for 11.4%, 8.0% and 3.9%, respectively) while motor vehicles contributed 10.1% (diesels 8.7% and gasoline vehicles 1.4%). Secondary sources for sulfates, nitrates, and organic aerosols accounted for ~41.5% of the $PM_{2.5}$ mass. A complementary analysis using the WRF-CHEM model showed that regional transport accounted for 60.8% of the $PM_{2.5}$ during the winter high-pollution period, which also implies the importance of secondary aerosols.

Keywords: Xixian new district, $PM_{2.5}$, CAS-HERM, WRF-CHEM

1 INTRODUCTION

Haze events, which are mainly caused by atmospheric fine particles, occur frequently in China, and air pollution in many parts of the country has impacted public health and impeded socioeconomic development (Huang *et al.*, 2014; An *et al.*, 2019). In fact, fine particles have become the main air pollutant of concern in many large and medium-sized cities in China, especially in autumn and winter when $PM_{2.5}$ concentrations can be greatly elevated (Cao, 2014; Huang *et al.*, 2014; An *et al.*, 2019). Fine particle matter, also known as $PM_{2.5}$, is small in size (≤ 2.5 μm aerodynamic equivalent diameter) but has a large specific surface area, which favors the adsorption of harmful substances. These $PM_{2.5}$ particles can stay suspended in the air for days to weeks, and they can enter the lungs and impair human health. In addition, increases in $PM_{2.5}$ mass concentrations reduce atmospheric visibility, thus affecting daily activities, including transportation. In-depth studies of $PM_{2.5}$ are a continuing need for improving China's environmental air quality (Cao, 2014; Zhang *et al.*, 2019b).

In 2018, the Fenwei Plain, which includes the Guanzhong basin (GZB), was listed as one of three priority areas of concern for air pollution in China (Zhai *et al.*, 2019). Numerous studies on the air pollution in the GZB and Shaanxi regions have been conducted (Cao *et al.*, 2005, 2012, Cao, 2014; Wang *et al.*, 2014; You *et al.*, 2015; Chen *et al.*, 2016; Xu *et al.*, 2016; Xu *et al.*, 2018), and the seriousness of air pollution in the GZB has become all too evident (Huang *et al.*, 2015; Li *et al.*, 2017). It has been shown, for example, that the $PM_{2.5}$ concentrations on hazy days were typically two times higher compared with non-hazy days, and $PM_{2.5}$ often exceeds the National Air Quality Standard value during haze events (Shen *et al.*, 2009; You *et al.*, 2015; Zhang *et al.*, 2015; Chen *et al.*, 2016; Zhang *et al.*, 2019a). The chemical components of the particles were also found to differ

OPEN ACCESS

Received: April 14, 2020
Revised: September 26, 2020
Accepted: September 26, 2020

* **Corresponding Authors:**
cao@loess.llqg.ac.cn

Publisher:
Taiwan Association for Aerosol Research
ISSN: 1680-8584 print
ISSN: 2071-1409 online

for hazy versus non-hazy days, and those differences were attributed to changes in the major sources and the effects of regional transport on pollutants.

The Xixian New District (XXND) is located in the Fenwei Plain, and it is the seventh national-level new district in China that was officially approved on January 6, 2014. The district is located between the main urban areas of Xi 'an and Xianyang, and it is expected to become the main functional new district and ecological center of the Xi'an metropolis. With the growing social, political and economic importance of XXND, environmental issues, especially $PM_{2.5}$ pollution, are of great concern. However, there has been little research on air pollution there, especially assessments of the sources for $PM_{2.5}$ in the region. The development of effective measure for controlling air pollution requires information on the sources of the pollutants, and in this paper, the sources for $PM_{2.5}$ in the XXND region were evaluated by using a source apportionment model (CAS-HERM) and a chemical transport model (WRF-CHEM). The objectives of this study were to (1) obtain the chemical characteristics of $PM_{2.5}$, (2) conduct a comprehensive analysis of the sources for $PM_{2.5}$, and (3) provide guidance for regulators and establish a reference point for assessments of air quality in the future. The Ministry of Ecology and Environment of China requires major cities in China to conduct refined source apportionments to support the needs of environmental managers. Here we use the term “refined apportionment” to indicate that the $PM_{2.5}$ dust sources were separated into construction, road, and soil dusts, while the motor vehicle source emissions were split between those from gasoline- and diesel-powered vehicles.

2. METHODS

2.1 Sample Collection and Analysis

Four routine monitoring sites were selected for the studies of $PM_{2.5}$ in the XXND by taking into account the distribution of functional areas, population density, environmental sensitivity, and prevailing wind directions. From north to south, the stations were as follows: Zhangjiashan (ZJS, 34.66°N, 108.59°E), Chongwen Pagoda (CWP, 34.50°N, 108.95°E), Meteorological Bureau (MB, 34.39°N, 108.71°E), and Fengdong New Town (FDNT, 34.26°N, 108.78°E) (see supplemental Fig. S1 and Text S1). The ZJS station is located in the north, far from urban areas and with no pollution sources nearby, and it was used as a background reference site. The CWP, MB, FDNT stations represent different urban areas of the XXND.

Our study involved one month of sample collection for $PM_{2.5}$ in each of four seasons from 2017 to 2018. The discussion of the chemical data for the filters is based on seasons defined as follows: December 18, 2017–January 21, 2018 as winter, April 27, 2018–May 25, 2018 as spring, July 25, 2018–August 22, 2018 as summer and October 31, 2018–November 29, 2018 as autumn. A micro-volume sampler, which operated at a flow rate of 5 L min^{-1}, was used to collect the filter samples. Each sample was pumped continuously for 24 h, and the monitoring period was from 10:00 am to 10:00 am of the next day. A total of 1016 $PM_{2.5}$ filter samples were collected, including 508 quartz filters and 508 Teflon™ filter membranes.

The mass concentrations of the $PM_{2.5}$ samples were determined gravimetrically with the use of a micro-electronic balance (ME 5-F, Sartorius, Göttingen, Germany). A thermal/optical carbon analyzer (Model 2001, Atmoslytic Inc., Calabasas, CA, USA) was used to measure the organic and elemental carbon components (OC and EC, respectively). An ion chromatograph (IC, Metrohm 940, Swiss Metrohm Group, Switzerland) was used to quantitatively analyze water-soluble ion concentrations (Cl^-, NO^{3-}, SO_4^{2-}, Na^+, NH_4^+, K^+, Mg^{2+}, Ca^{2+}). Eighteen elements (Na, Mg, Al, Si, S, Cl, K, Ca, Ti, Mn, Fe, Cu, Zn, As, Br, Sr, Ba, Pb) in the filter were analyzed by energy dispersive X-ray fluorescence analyzer (ED-XRF) (Epsilon 4, PANalytical B.V., the Netherlands).

2.2 Source Apportionment of $PM_{2.5}$ with the CAS-HERM Receptor Model

A comprehensive receptor source apportionment model (CAS Hybrid Environmental Receptor Model, CAS-HERM) developed by the Institute of Earth Environment, Chinese Academy of Sciences, and based on positive matrix factorization (PMF) and chemical mass balance (CMB) receptor models, was used to identify likely pollution sources for the $PM_{2.5}$.

The CAS-HERM model combines the advantages of PMF and CMB models, and it can simulate situations in which the source spectrum is known, unknown, or partially known (Chen and Cao,

2018). The principles of the model are explained in Supplemental Text S2. The data input into the model included the $PM_{2.5}$ chemical component concentrations and uncertainties. We used CAS-HERM to calculate reduced chi-squared values, which are useful for identifying the number of sources, and we used the known source profiles to run that model. Most of source profiles were taken from a database of source profiles in China (http://www.sourceprofile.org.cn) (Cao, 2018). Source profiles for dust and motor exhaust were adopted from other studies made by our group. Table S1 contains information on the source profiles and five primary source profiles adapted in the study. The methods for calculating uncertainties and details concerning the model input data can be found in Chen and Cao (2018). The criteria that were used to select the results for discussion included linear fitting of observed versus fitted $PM_{2.5}$ concentrations. If the slope and coefficients of determination (R^2) of linear fitting result were close to one (Fig. S2 in the supplementary), the model result was considered reasonable.

2.3 Simulation Using the WRF-CHEM Model

As the contributions of local versus remote emission sources cannot be resolved by receptor models, including the CAS-HERM, a chemical transport model was employed for that purpose. The Weather Research and Forecast Model with Chemistry (WRF-CHEM) model developed by Grell *et al.* (2005) was adopted for our work, and as used, it was fully coupled with online weather research and forecasts. Real-time, on-line feedbacks between meteorological and chemical processes are a feature of the model, which previously has been used for atmospheric pollution simulations in the GZB (Li *et al.*, 2017). The simulations in our study focus on persistent pollution events in the XXND, which lasted from December 30, 2017 to January 30, 2018. The goal for the exercise was to evaluate the relative contributions of local versus remote emission sources during the highest $PM_{2.5}$ season. The base year of the emission inventory used for the model was 2009, and it was updated in 2017, based on an inventory survey for this project. Five major sources (industrial, power plants, residential, transportation, and agriculture) were included in the emission inventory and the spatial resolution of the model was ~6 km. A detailed description about the WRF-CHEM modeling may be found in Text S3.

3. RESULTS AND DISCUSSION

3.1 Chemical Characteristics of $PM_{2.5}$ in the Xixian New District

The annual average concentration of $PM_{2.5}$ in XXND during the monitoring period was 67 ± 39 μg m^{-3}, which is considerably higher than the annual average concentration listed in the National Air Quality Standard (35 μg m^{-3}). The seasonal results summarized in Table 1 show that the $PM_{2.5}$ mass concentrations (arithmetic mean ± standard deviation) decreased from winter (119 ± 55 μg m^{-3}) to autumn (75 ± 47 μg m^{-3}) to spring (44 ± 22 μg m^{-3}), and finally summer (31 ±10 μg m^{-3}). Monthly averages for $PM_{2.5}$ in winter were about four times of those in summer, and the highest daily $PM_{2.5}$ mass loading exceeded 250 μg m^{-3}. These high concentrations reflect the seriousness of particulate pollution, especially in the winter.

In general, most of the main chemical components of $PM_{2.5}$ showed the same seasonal patterns as the mass concentrations; that is, high concentrations and large variations in winter compared with lower, less variable concentrations in summer (Table 1). Of all chemical components, OC, nitrate and sulfate were the three most abundant species (Table 1), accounting for 18.2%, 17.0%, and 13.1% of the annual mass concentrations, respectively. The OC and EC concentrations in $PM_{2.5}$ followed similar seasonal patterns; that is, winter > autumn > spring > summer. High OC and EC concentrations have been associated with emissions that result from residential heating in winter (Cao *et al.*, 2005). The sum of eight ions (Cl^-, NO_3^-, SO_4^{2-}, Na^+, NH_4^+, K^+, Mg^{2+}, Ca^{2+}) accounted 44.8% of the annual $PM_{2.5}$ loadings. Of these, the three most abundant species, NO_3^-, SO_4^{2-}, NH_4^+, accounted for 17.0%, 13.1%, and 6.9% of the mass, respectively. The highest concentrations of secondary inorganic ions occurred in winter when NO_3^- showed the highest mean loadings (21.9 μg m^{-3}), followed by SO_4^{2-} (14.2 μg m^{-3}) and NH_4^+ (9.9 μg m^{-3}). The concentrations of nitrate exceeded those of sulfate in the winter, which is an indication of the increasing importance of NO_x emission and the efficiency of SO_2 controls in winter (Shen *et al.*, 2008; Xu *et al.*, 2016). In summer, however, the sulfate concentrations exceeded those of nitrate (Table 1).

Table 1. Seasonal and annual concentrations (arithmetic mean ± standard deviation) of $PM_{2.5}$ and chemical components (μg m^{-3}) from the Xixian New District.

Species	Winter	Spring	Summer	Autumn	Annual
$PM_{2.5}$	119 ± 55	44 ± 22	31 ± 10	75 ± 47	67 ± 39
Organic carbon	25.2 ± 12.9	6.5 ± 3	4.3 ± 1.7	13 ± 7.1	12.2 ± 9.4
Elemental carbon	6.0 ± 3.5	1.9 ± 1.2	1.6 ± 0.9	5.3 ± 3.4	3.7 ± 2.3
Cl^-	3.6 ± 2.9	0.4 ± 0.3	0.2 ± 0.2	1.2 ± 1	1.3 ± 1.6
NO_3^-	21.9 ± 15.9	5 ± 5.5	2.8 ± 1.2	15.9 ± 13	11.4 ± 9
SO_4^{2-}	14.2 ± 9.2	5.8 ± 2.5	8.8 ± 3.9	6.6 ± 3.8	8.8 ± 3.8
Na^+	0.9 ± 0.7	1.8 ± 0.9	1.7 ± 1.0	1.5 ± 0.9	1.5 ± 0.4
NH_4^+	9.9 ± 7.4	1.2 ± 1.7	1.7 ± 1.3	5.5 ± 4.6	4.6 ± 4.1
K^+	1.4 ± 0.9	0.1 ± 0.2	0.1 ± 0.1	0.7 ± 0.4	0.6 ± 0.6
Mg^{2+}	0.1 ± 0.1	0.4 ± 0.2	0.2 ± 0.2	0.2 ± 0.2	0.2 ± 0.1
Ca^{2+}	1.1 ± 1.3	1.9 ± 1.5	1.8 ± 1.6	1.5 ± 2.2	1.6 ± 0.4
Na	0.71 ± 0.44	0.06 ± 0.1	0.25 ± 0.15	0.41 ± 0.34	0.36 ± 0.28
Mg	0.47 ± 0.35	0.31 ± 0.26	0.29 ± 0.14	0.41 ± 0.48	0.37 ± 0.09
Al	1.01 ± 1.01	1.01 ± 0.8	0.32 ± 0.1	0.83 ± 1.5	0.8 ± 0.33
Si	2.15 ± 2.45	2.35 ± 1.98	0.48 ± 0.17	1.75 ± 3.68	1.68 ± 0.84
S	3.79 ± 2.22	1.43 ± 0.69	2.69 ± 1.25	1.74 ± 0.96	2.41 ± 1.06
Cl	2.89 ± 2.12	0.14 ± 0.19	0.02 ± 0.02	0.99 ± 0.83	1.01 ± 1.32
K	2.14 ± 1.13	0.91 ± 0.45	0.51 ± 0.14	1.33 ± 1.00	1.22 ± 0.70
Ca	1.55 ± 1.67	1.6 ± 1.57	0.38 ± 0.19	1.18 ± 1.99	1.18 ± 0.56
Ti	0.08 ± 0.08	0.09 ± 0.07	0.02 ± 0.01	0.06 ± 0.12	0.06 ± 0.03
Mn	0.05 ± 0.03	0.03 ± 0.02	0.01 ± 0.01	0.03 ± 0.04	0.03 ± 0.02
Fe	1.00 ± 0.90	1.02 ± 0.79	0.29 ± 0.13	0.95 ± 1.51	0.81 ± 0.35
Cu	0.01 ± 0.01	0.01 ± 0.02	n.d.[1]	0.01 ± 0.01	0.01 ± 0.01
As	0.01 ± 0.01	n.d.	n.d.	0.01 ± 0.00	0.01 ± 0.00
Br	0.02 ± 0.02	n.d.	n.d.	0.01 ± 0.01	0.01 ± 0.01
Sr	0.01 ± 0.01	0.01 ± 0.01	n.d.	0.01 ± 0.01	0.01 ± 0.00
Ba	0.01 ± 0.01	0.01 ± 0.02	n.d.	0.01 ± 0.01	0.01 ± 0.00
Pb	0.07 ± 0.05	0.03 ± 0.02	0.03 ± 0.01	0.04 ± 0.03	0.04 ± 0.02
Zn	0.2 ± 0.16	0.12 ± 0.09	0.08 ± 0.04	0.14 ± 0.1	0.13 ± 0.05

[1] n.d. stands for < minimum detection limit.

The highest concentrations of Cl^- and K^+ (3.6 and 1.4 μg m^{-3}, respectively) were likely due to the burning of large quantities of coal and biomass in winter for heating, whereas ions that typically are associated with dust (Mg^{2+}, Ca^{2+}) were relatively high in spring (0.1 μg m^{-3}, 1.1 μg m^{-3}). Table 1 shows the concentrations of eight elements (Al, Si, S, Ti, Mn, Fe, Pb and Zn) in $PM_{2.5}$ from XXND, including five elements (Cu, As, Br, Sr and Ba) that were detected in only trace amounts. Of the elements measured, Al, Si, Fe and Ti are representative of mineral dust (Cao *et al.*, 2012; Chen and Cao, 2018), and they decreased with season as follows: spring > winter > autumn > summer. The loadings of Zn, Pb and Mn, which are largely anthropogenic (Cao *et al.*, 2012; Chen and Cao, 2018), decreased from winter > autumn > spring > summer while those for S decreased from winter > summer > autumn > spring.

3.2 Sources for $PM_{2.5}$ in the Xixian New District

The source contributions to $PM_{2.5}$ at the four stations in XXND (FDNT, CWP, MB and ZJS) were resolved using CAS-HERM receptor model. All of the coefficients of determination (R^2) between the observed and fitted $PM_{2.5}$ values were > 0.96, and the ratios of fitted to observed values were close to unity, indicating that the source apportionment results were reasonable (see Fig. S2). The spatio-temporal changes in the pollution sources for $PM_{2.5}$ were assessed with the model, and the results are shown in Fig. 1. The $PM_{2.5}$ masses at all four stations had the largest contributions from secondary pollution sources—the combined annual percent contributions of secondary sulfate and secondary OC was ~30%, and the combined annual contribution of secondary nitrate

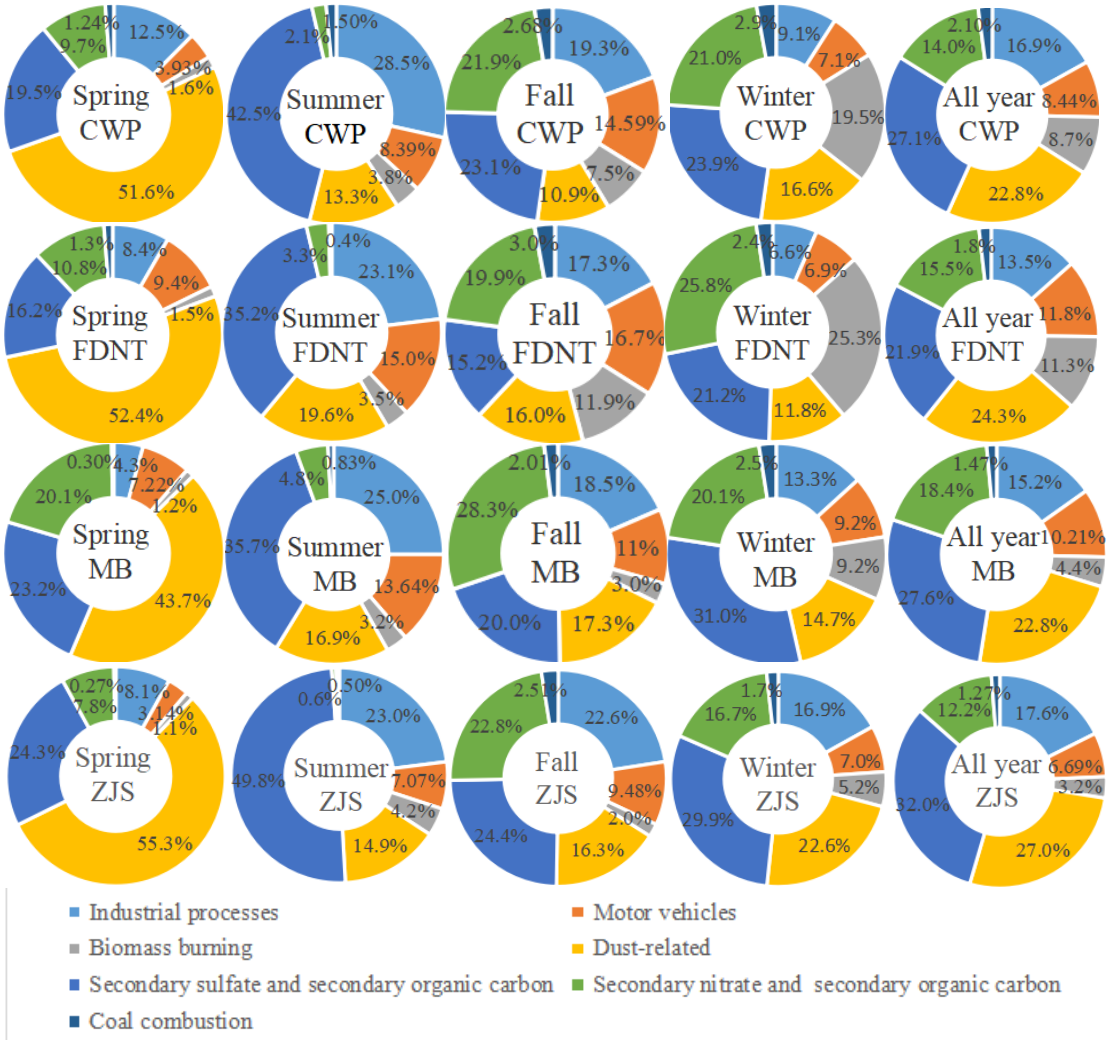

Fig. 1. Seasonal and annual source apportionments for $PM_{2.5}$ from four monitoring stations in the Xixian New District.

and secondary OC was ~15%. We note that secondary sources mainly reflect the contributions from regional pollution sources possibly in combination with influences from even more remote sources.

Primary sources are often associated with local emissions, and the contributions from dust and industrial process sources were moderate and relatively similar, ~20% and 15% respectively. The annual contributions from motor vehicle sources at the CWP, FDNT and MB stations were ~10%, but their influence was lower at the ZJS station (6.7%), presumably because of the greater distance between that station and urban centers and the small number of motor vehicles in the area. The contribution of biomass burning sources was ~10% annually at CWP and FDNT, while at MB and ZJS, the impacts from biomass burning were even lower, only ~5%. This is likely because CWP and FDNT are closer to suburban districts and counties, and so the impacts from biomass burning are more significant. The contribution of coal combustion to the primary $PM_{2.5}$ at all stations was relatively low, only ~2%, but secondary particles, including those resulting from coal combustion were important.

In terms of seasonality, the most prominent pollution sources contributing to $PM_{2.5}$ in spring were dust related (43.7%–55.3%), secondary sulfate and secondary OC (16.2%–24.3%) as described in supplemental text S2 and illustrated in Fig. 1. The main $PM_{2.5}$ particle types in summer were secondary sulfate and secondary OC (35.2%–49.8%), and large impacts from industrial processes were evident (23.0%–28.5%). In autumn, the contributions of the various pollution sources were relatively uniform, and the $PM_{2.5}$ was distributed as follows (see supplemental text S2): secondary nitrate and secondary OC (19.9%–28.3%) as described in

supplemental text S2, secondary sulfate and secondary OC (15.2%–24.4%), industrial processes (17.3%–22.6%), and dust production (10.9%–17.3%). In winter, the source contributions to $PM_{2.5}$ followed the order secondary sulfate and secondary OC (21.2%–31.0%), secondary nitrate and secondary OC (16.7%–25.8%), dust–related sources (11.8%–22.6%), and biomass burning (5.2%–25.3%).

3.3 Influences from Local versus Regional Sources

Winter is the most polluted season in the XXND, and therefore, to reduce the average annual loadings of pollutants, the implementation of controls in winter would a logical first step in addressing the air pollution problem. The CAS-HERM receptor model is not able to distinguish between the contributions from local versus regional sources, and therefore, we used the WRF-CHEM model to investigate this issue. Fig. 2 shows the spatial distributions of the observed and simulated mean mass concentrations of $PM_{2.5}$, O_3, NO_2, and SO_2 at GZB in the winter of 2017, and Fig. S4 shows time-series plots of the observed and simulated hourly mass concentrations of these same chemical species. In general, the WRF-CHEM model reproduced the temporal variations and spatial distributions of the major air pollutants reasonably well. In terms of the latter, most areas of XXND experienced heavy pollution during the simulation period when the $PM_{2.5}$ mass concentrations ranged from 150 to 250 μg m^{-3}. The WRF-CHEM model also simulated the spatial distributions of O_3, NO_2 and SO_2 quite well. Indeed, the model reproduced the

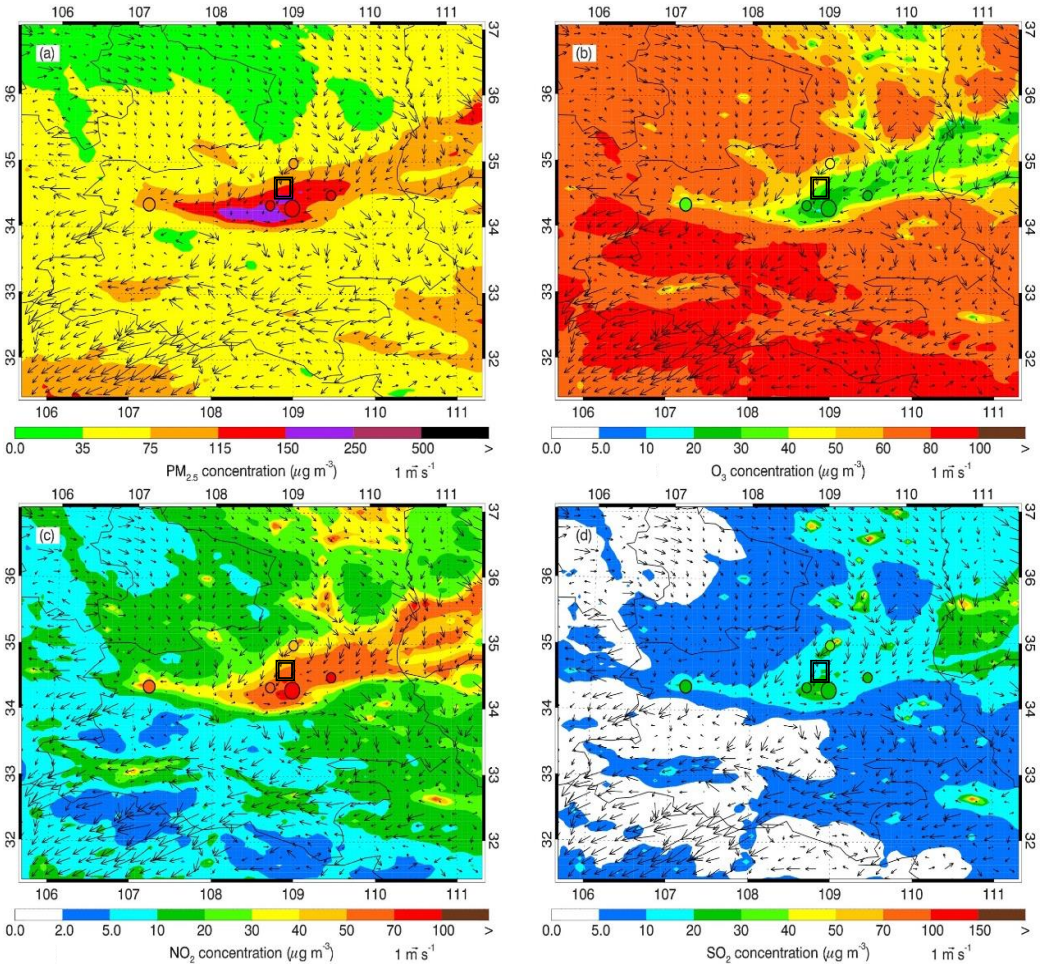

Fig. 2. Spatial distributions of mean mass concentrations of (a) $PM_{2.5}$, (b) O_3, (c) NO_2, and (d) SO_2 in the Guanzhong basin from December 30, 2017 to January 30, 2018. The rectangular box represents the XXND. Colored circles represent the average $PM_{2.5}$ observations in five cities at Guanzhong basin (Xi'an, Xianyang, Baoji, Weinan, and Tongchuan). Color contours are $PM_{2.5}$ average simulations. Black arrows indicate simulated surface winds.

temporal variations and spatial distributions of the major $PM_{2.5}$ air pollutants with considerable accuracy because the differences between the simulated and observed values were only ~5–10%. We note that in addition to the difficulties in accurately representing meteorological conditions, especially boundary layer height and horizontal wind fields, uncertainties in the emissions likely affected the accuracy of the model simulations.

Overall, local emissions had a relatively minor impact on $PM_{2.5}$ pollution levels in XXND: the contribution of local emissions to the total mass loadings was between 20–40 μg m^{-3} during the heavy pollution period. Rather, $PM_{2.5}$ pollution in XXND was dominated by transport because particles that originated from outside the region could account for 60–100 μg m^{-3} of the total $PM_{2.5}$ mass. The methods used for this assessment may be found in supplemental Text S3, and the results presented in Table 2 show the contributions of local emissions versus transport to the major air pollutants during the simulation. The average mass concentration of $PM_{2.5}$ in XXND during the simulation period was 147.1 μg m^{-3}, which is a moderate to heavily polluted level, and the background concentration was 16.2 μg m^{-3}, which is equivalent to ~11.0% of the total $PM_{2.5}$ mass. Over the course of simulation, regional transport played a dominant role in the particulate air pollution because that accounted for an estimated ~60.8% (89.5 μg m^{-3}) of the $PM_{2.5}$ mass, compared with only 19.8% (29.2 μg m^{-3}) from local XXND sources. Meanwhile, interactions between background $PM_{2.5}$ local emissions and regional transportation increased the $PM_{2.5}$ mass concentration by about 8.4% (12.2 μg m^{-3}).

3.4 Refined Source Apportionment of $PM_{2.5}$ in XXND

For our study, refined source apportionments were used to first separate the contributions dust and motor vehicles to $PM_{2.5}$ mass concentrations. The dust-related sources were then further divided into three categories: construction, road, and soil dust using the CAS-HERM model (the methodology is presented in the supplementary material). Similarly, motor vehicle emission sources were separated into those from petrol- versus diesel-powered vehicles, using the 2018 motor vehicle emergency emission reduction inventory data for Xi'an. Detailed results of refined source contributions of $PM_{2.5}$ are shown in Fig. 3. For the primary pollutants, the contributions from dust-related sources and industrial processes were significant, accounting for 23.3% and 15.2% of the $PM_{2.5}$ mass, respectively. The percentages of $PM_{2.5}$ attributed to road dust, construction dust and soil dust (including emissions from farmlands) in the dust-related source were 11.4%, 8.0% and 3.9% respectively. The contribution from motor vehicles was 10.1% and biomass burning was 8.1%. Diesel-powered vehicles accounted for more than 85% of the emissions from motor vehicles and 8.7% of the total emissions. The annual contribution of coal combustion to the primary $PM_{2.5}$ in XXND was relatively low, only 1.8%, but that does not mean that the contribution of coal combustion sources to $PM_{2.5}$ was not important. This is because sulfur dioxide, nitrogen oxides, and volatile organic compounds emitted from coal combustion sources can be converted into secondary sulfate, nitrate and organic aerosols.

In fact, secondary pollutants (nitrate, sulfate, and organic matter) accounted for a large percentage (41.5%) of the $PM_{2.5}$ mass (Fig. 3). In addition to gas-to-particle conversion of precursor gases from coal combustion, some of the secondary species were likely produced from NH_3 emitted from farmlands and livestock and from VOCs that originated from numerous widespread sources. These findings are consistent with the WRF-CHEM model results presented above which showed that regional transport accounted for 60.8% of $PM_{2.5}$ during the high-pollution events in

Table 2. Contributions of local emissions and regional transport to the main air pollutants in the Xixian New District. See Table S3 for detailed experimental design details. The interaction term represents the interactions between background, local emissions and regional transport.

Model	$PM_{2.5}$ mass concentration	
	(μg m^{-3})	Percentage
Background concentration	16.2	11.0%
Local emissions	29.2	19.8%
Regional transport	89.5	60.8%
Interaction	12.2	8.4%

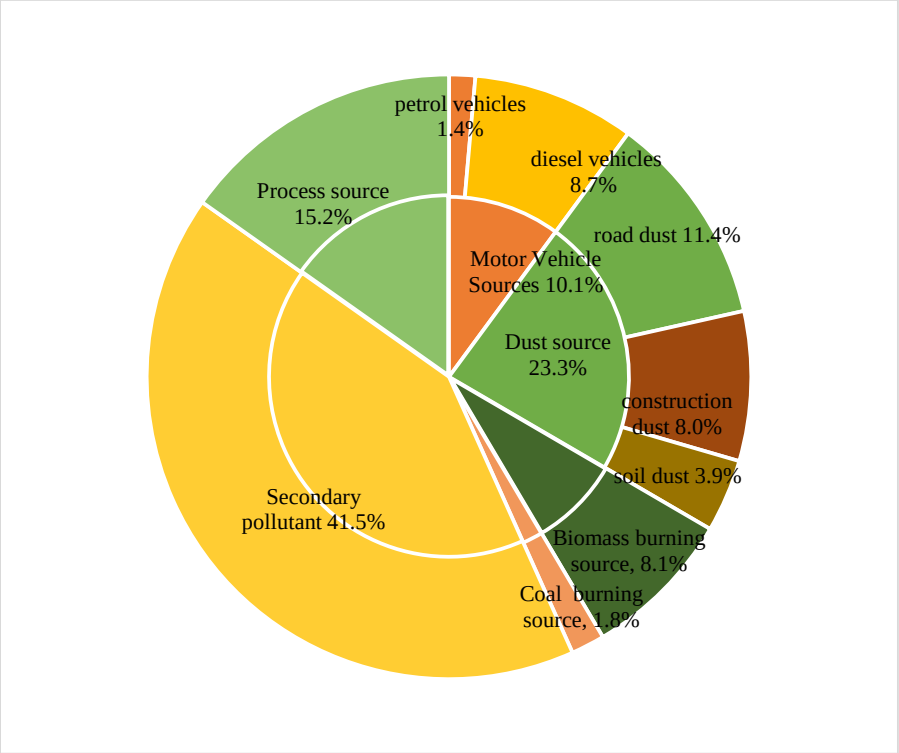

Fig. 3. Source apportionments of $PM_{2.5}$ from the Xixian New District. The inner circle shows the general results and the outer circle shows the more refined results.

the winter. Dust sources were not included in the current WRF-CHEM modelling, however, and the contribution from regional sources likely would have been lower than 60.8% if we had been able to include that dust component of the $PM_{2.5}$. In a study in Beijing, for instance, most of the dust was found to be associated with local emissions (Han *et al.*, 2007). The percentage of $PM_{2.5}$ mass from secondary aerosols obtained from the receptor models (41.5%) can explain much of the regional contribution to the pollution aerosol over the annual scale.

As XXND is a new district, there have been no previous source apportionments available for this area, so we compared our results with previous studies in the nearby city of Xi'an from 2006 to 2010 (Xu *et al.*, 2016). Compared with Xi'an, the dust fraction of $PM_{2.5}$ mass at XXND was considerably higher (Table 3). This is can be explained by large number of construction sites for buildings and roads in the new district; indeed, the dust faction of the $PM_{2.5}$ mass was as high as 23.3%. Industrial sources also showed a stronger impact in XXND compared with Xi'an in that period; this can be explained by several large industrial sources in XXND, including petrochemical plants, methanol plants, etc. The proportion of $PM_{2.5}$ mass assigned to motor vehicles in XXND was about half that at Xi'an, which is probably because XXND is a new and developing urban area, and the number of motor vehicles in use is lower than in Xi'an. Biomass burning in XXND was 2 to 3% percent higher than in Xi'an, and that is probably related to the more rural character of XXND. The proportion of coal burning in XXND was much lower than in Xi'an in 2006–2010, most likely because the local government has strictly reduced coal consumption in recent years. The secondary aerosol pollutants in XXND accounted for a larger proportion (41.5%) of the $PM_{2.5}$ mass than in Xi'an, and that can be explained by the large impacts from areas surrounding XXND. In fact, the area of the XXND is about one tenth of the area of Xi'an, and therefore, it is more likely to be affected by pollution transport from surrounding areas.

4 CONCLUSIONS

This study focused on the characteristics and sources of $PM_{2.5}$ in the Xixian New District from 2017 to 2018, and the results obtained for the first refined source apportionment showed that

Table 3. Comparison of source apportionment results at Xixian New District and Xi'an.

Site	Xian			XiXian New District
Year	2006	2008	2010	2018
Source category	%	%	%	%
Fugitive dust	12.8	11.7	19.4	23.3
Industrial emissions	9.8	11.5	12.6	15.2
Motor vehicle emissions	19.3	20.9	21.3	10.1
Biomass burning emissions	6	5.1	5.1	8.1
Coal combustion emissions	31.2	27.6	24.1	1.8
Secondary aerosol pollutants	20.9	23.2	17.5	41.5

primary sources accounted for ~58.5% of the $PM_{2.5}$ mass. These sources were associated with dust production, industrial emissions, motor vehicles, and biomass combustion, and a relatively high proportion of the primary particles could be traced to pollution emissions. Dust accounted for 23.3% of the $PM_{2.5}$, and of that, road dust, construction dust, and soil dust accounted for 11.4%, 8.0% and 3.9% of the total mass, respectively. Together, road dust and construction dust accounted for ~20% of $PM_{2.5}$, and these two sources should be controlled to address the $PM_{2.5}$ pollution problems. Motor vehicles accounted for 10.1% of $PM_{2.5}$ mass, of which diesel vehicles and gasoline vehicles accounted for 8.7% and 1.4%, respectively. Therefore, diesel vehicles should be the first focus for motor vehicle pollution controls in this district. Coal combustion accounted for only 1.8% of the primary particles, and that small impact is undoubtedly related to the sharp decline in coal usage in recent years. Secondary sources for $PM_{2.5}$ accounted for ~41.5% of the $PM_{2.5}$ mass, and the secondary particles were mainly sulfates, nitrates, and organic aerosols. WRF-CHEM model simulations for the winter, high-pollution season showed that the regional transport could account for 60.8% of the $PM_{2.5}$: this is consistent with the results from the receptor model which indicated that secondary sources were responsible for a large percentage (41.5%) of the $PM_{2.5}$ mass. The information regarding $PM_{2.5}$ and results of the refined source apportionment obtained from this study can provide guidance for the prioritization of pollution controls and can serve as a reference for future assessments of air quality.

ACKNOWLEDGEMENTS

This research was supported by the special project of joint prevention and control of air pollution in Guanzhong of Shaanxi province (2017YFC0212200) and Xianyang source apportionment project.

SUPPLEMENTARY MATERIAL

Supplementary data associated with this article can be found in the online version at https://doi.org/10.4209/aaqr.2020.04.0146

REFERENCES

An, Z., Huang, R.-J., Zhang, R., Tie, X., Li, G., Cao, J., Zhou, W., Shi, Z., Han, Y., Gu, Z., Ji, Y. (2019). Severe haze in northern China: A synergy of anthropogenic emissions and atmospheric processes. PNAS 116, 8657–8666. https://doi.org/10.1073/pnas.1900125116

Cao, J.J., Wu, F., Chow, J.C., Lee, S.C., Li, Y., Chen, S.W., An, Z.S., Fung, K.K., Watson, J.G., Zhu, C.S., Liu, S.X. (2005). Characterization and source apportionment of atmospheric organic and elemental carbon during fall and winter of 2003 in Xi'an, China. Atmos. Chem. Phys. 5, 3127–3137. https://doi.org/10.5194/acp-5-3127-2005

Cao, J.J., Shen, Z.X., Chow, J.C., Watson, J.G., Lee, S.C., Tie, X.X., Ho, K.F., Wang, G.H., Han, Y.M. (2012). Winter and summer $PM_{2.5}$ chemical compositions in fourteen Chinese cities. J. Air Waste Manage. Assoc. 62, 1214–1226. https://doi.org/10.1080/10962247.2012.701193

Cao, J.J. (2014). $PM_{2.5}$ and environment, Science Press, pp. 6–18.

Cao, J.J. (2018). A brief introduction and progress summary of the $PM_{2.5}$ source profile compilation project in China. Aerosol Sci. Eng. 2, 43–50. https://doi.org/10.1007/s41810-018-0026-4

Chen, L.W.A., Cao, J.J. (2018). $PM_{2.5}$ source apportionment using a hybrid environmental receptor model. Environ. Sci. Technol. 52, 6357-6369. https://doi.org/10.1021/acs.est.8b00131

Chen, Y., Cao, J., Huang, R., Yang, F., Wang, Q., Wang, Y. (2016). Characterization, mixing state, and evolution of urban single particles in Xi'an (China) during wintertime haze days. Sci. Total. Environ. 573, 937–945. https://doi.org/10.1016/j.scitotenv.2016.08.151

Grell, G.A., Peckham, S.E., Schmitz, R., McKeen, S.A., Frost, G., Skamarock, W.C., Eder, B. (2005). Fully coupled "online" chemistry within the WRF model. Atmos. Environ. 39, 6957–6975. https://doi.org/10.1016/j.atmosenv.2005.04.027

Han, L., Zhuang, G., Cheng, S., Wang, Y., Li, J. (2007). Characteristics of re-suspended road dust and its impact on the atmospheric environment in Beijing. Atmos. Environ. 41, 7485–7499. https://doi.org/10.1016/j.atmosenv.2007.05.044

Huang, P., Zhang, J., Tang, Y., Liu, L. (2015). Spatial and temporal distribution of $PM_{2.5}$ pollution in Xi'an City, China. Int. J. Environ. Res. Public Health 12, 6608–6625. https://doi.org/10.3390/ijerph120606608

Huang, R.J., Zhang, Y., Bozzetti, C., Ho, K.F., Cao, J.J., Han, Y., Daellenbach, K.R., Slowik, J.G., Platt, S.M., Canonaco, F., Zotter, P., Wolf, R., Pieber, S.M., Bruns, E.A., Crippa, M., Ciarelli, G., Piazzalunga, A., Schwikowski, M., Abbaszade, G., … Zotter, P (2014). High secondary aerosol contribution to particulate pollution during haze events in China. Nature 514, 218–222. https://doi.org/10.1038/nature13774

Li, G., Bei, N., Cao, J., Huang, R., Wu, J., Feng, T., Wang, Y., Liu, S., Zhang, Q., Tie, X., Molina, L.T. (2017). A possible pathway for rapid growth of sulfate during haze days in China. Atmos. Chem. Phys. 17, 3301–3316. https://doi.org/10.5194/acp-17-3301-2017

Shen, Z., Arimoto, R., Cao, J., Zhang, R., Li, X., Du, N., Okuda, T., Nakao, S., Tanaka, S. (2008). Seasonal Variations and Evidence for the Effectiveness of Pollution Controls on Water-Soluble Inorganic Species in Total Suspended Particulates and Fine Particulate Matter from Xi'an, China. J. Air Waste Manage. Assoc. 58, 1560–1570. https://doi.org/10.3155/1047-3289.58.12.1560

Shen, Z., Cao, J., Arimoto, R., Han, Z., Zhang, R., Han, Y., Liu, S., Okuda, T., Nakao, S., Tanaka, S. (2009). Ionic composition of TSP and $PM_{2.5}$ during dust storms and air pollution episodes at Xi'an, China. Atmos. Environ. 43, 2911–2918. https://doi.org/10.1016/j.atmosenv.2009.03.005

Wang, D., Hu, J., Xu, Y., Lv, D., Xie, X., Kleeman, M., Xing, J., Zhang, H., Ying, Q. (2014). Source contributions to primary and secondary inorganic particulate matter during a severe wintertime $PM_{2.5}$ pollution episode in Xi'an, China. Atmos. Environ. 97, 182–194. https://doi.org/10.1016/j.atmosenv.2014.08.020

Xu, H., Cao, J., Chow, J.C., Huang, R.J., Shen, Z., Chen, L.W.A., Ho, K.F., Watson, J.G. (2016). Inter-annual variability of wintertime $PM_{2.5}$ chemical composition in Xi'an, China: Evidences of changing source emissions. Sci. Total. Environ. 545–546, 546–555. https://doi.org/10.1016/j.scitotenv.2015.12.070

Xu, Y., Ying, Q., Hu, J., Gao, Y., Yang, Y., Wang, D., Zhang, H. (2018). Spatial and temporal variations in criteria air pollutants in three typical terrain regions in Shaanxi, China, during 2015. Air Qual. Atmos. Health 11, 95–109. https://doi.org/10.1007/s11869-017-0523-7

You, W., Zang, Z., Pan, X., Zhang, L., Chen, D. (2015). Estimating $PM_{2.5}$ in Xi'an, China using aerosol optical depth: A comparison between the MODIS and MISR retrieval models. Sci. Total. Environ. 505, 1156–1165. https://doi.org/10.1016/j.scitotenv.2014.11.024

Zhai, S., Jacob, D.J., Wang, X., Shen, L., Li, K., Zhang, Y., Gui, K., Zhao, T., Liao, H. (2019). Fine particulate matter ($PM_{2.5}$) trends in China, 2013–2018: Separating contributions from anthropogenic emissions and meteorology. Atmos. Chem. Phys. 19, 11031–11041. https://doi.org/10.5194/acp-19-11031-2019

Zhang, K., de Leeuw, G., Yang, Z., Chen, X., Su, X., Jiao, J. (2019a). Estimating Spatio-temporal variations of $PM_{2.5}$ concentrations using VIIRS-Derived AOD in the Guanzhong Basin, China. Remote Sens. 11, 2679. https://doi.org/10.3390/rs11222679

Zhang, Q., Shen, Z., Cao, J., Zhang, R., Zhang, L., Huang, R.J., Zheng, C., Wang, L., Liu, S., Xu, H., Zheng, C., Liu, P. (2015). Variations in $PM_{2.5}$, TSP, BC, and trace gases (NO_2, SO_2, and O_3) between

haze and non-haze episodes in winter over Xi'an, China. Atmos. Environ. 112, 64–71. https://doi.org/10.1016/j.atmosenv.2015.04.033

Zhang, Q., Zheng, Y., Tong, D., Shao, M., Wang, S., Zhang, Y., Xu, X., Wang, J., He, H., Liu, W., Ding, Y., Lei, Y., Li, J., Wang, Z., Zhang, X., Wang, Y., Cheng, J., Liu, Y., Shi, Q., … Hao, J. (2019). Drivers of improved PM2.5 air quality in China from 2013 to 2017. PNAS 116, 24463–24469. https://doi.org/10.1073/pnas.1907956116